Time-Dependent Sensitivity Analysis of OECD Benchmark using BISON and RAVEN

Paul W. Talbot[*†], *Kyle Gamble*[‡], *C. Rabiti*[†], *C. Wang*[†], *A. Alfonsi*[†], *J. J. Cogliati*[†], *D. Mandelli*[†], *A. K. Prinja*[*]

[*]*Department of Nuclear Engineering, University of New Mexico, Albuquerque, NM, 87131*
[†]*Nuclear Engineering Methods Development, Idaho National Laboratory, Idaho Falls, ID, 83415*
[‡]*Fuel Modeling and Simulation, Idaho National Laboratory, Idaho Falls, ID, 83415*
paul.talbot@inl.gov

INTRODUCTION

Developments in uncertainty quantification for nuclear simulations have decreased the computational cost required to perform accurate sensitivity analysis [1, 2, 3, 4]. This work demonstrates implementation of these methods in the RAVEN [5] framework, allowing for time-dependent sensitivity analysis. By demonstration we consider an OECD benchmark case [6]. We propagate uncertainties using RAVEN operating on the BISON [7] fuels performance code. We then consider the time-evolution of output response sensitivity to uncertain inputs. We perform sensitivity analysis using time-based stochastic collocation for generalized polynomial chaos (SCgPC) and high-dimension model reduction (HDMR) [8]. While uncertainty quantification applied to end-of-cycle statistics is useful, we demonstrate that dominant sources of uncertainty for figures of merit may fluctuate throughout the simulation. Time-dependent sensitivity analysis allows more insight on key design parameters for fuel.

METHODS

The details of the OECD benchmark and its parameter uncertainties are described in [6]. The benchmark includes a fuel pin in a steady-state PWR with power transients over a 2000 day period. During this time there is a power ramp up, then two steps down in power. Uncertain parameters include fuel properties, boundary conditions, and geometries. We treat each of the uncertain inputs as independent parameters and consider here four responses: maximum centerline fuel temperature, maximum clad creep strain, fission gas release percent, and clad elongation. The input parameters and distributions are in Table I.

TABLE I: Uncertain Parameters

Parameter	Mean	Std. Dev.	Units
clad cond.	16	2.5	W/m-K
clad thick	6.7e-4	8.3e-6	m
clad rough	5e-7	1e-7	m
creep rate	1	0.15	s^{-1}
fuel cond.	1	0.05	W/m-K
fuel dens.	10299.24	51.4962	kg/m^3
fuel exp.	1e-5	7.5e-7	
fuel radius	4.7e-3	3.335e-6	m
fuel swell	5.58e-5	5.77e-6	
gap cond.	1	0.025	W/m-K
gap width	9e-5	8.33e-6	m
mass flux	3460	57.67	kg/m^2s
rod pressure	1.2e6	4e4	Pa
sys pressure	1.551e7	51648.3	Pa
power scaling	1	0.016667	
Parameter	Low	High	Units
inlet temp	558	564	K

For propagation of uncertainty we use the high-dimension model reduction (HDMR) expansion [9],

$$u(Y) = u_0 + \sum_{n=1}^{N} u_n + \sum_{n_1=1}^{N} \sum_{n_2=1}^{n_1-1} u_{n_1,n_2} + \cdots, \tag{1}$$

where $u(Y)$ is the response as a function of inputs $Y = (y_1, \ldots, y_N)$, N is the dimensionality of the input space, and the components u_i are defined as

$$u_0 \equiv \int \cdots \int u(Y)\rho(Y)dY, \tag{2}$$

$$u_1 \equiv \int \cdots \int u(Y)\rho(y_2, \cdots, y_N)dy_2 \cdots dy_N, \tag{3}$$

$$u_{1,2} \equiv \int \cdots \int u(Y)\rho(y_3, \cdots, y_N)dy_3 \cdots dy_N, \tag{4}$$

and so forth, where $\rho(Y)$ is the joint probability distribution function of Y. Each of the terms in Eq. 1 can be represented using a generalized polynomial chaos expansion (gPC),

$$u(Y) \approx \sum_{k \in \Lambda} c_k \Phi_k(Y), \tag{5}$$

where Φ_k are multidimensional orthonormal polynomials of order $k = (k_1, \ldots, k_N)$ and Λ is a set of multi-index polynomial orders. Scalars c_k are given using sparse-grid collocation numerical integration [10],

$$c_k = \int \cdots \int u(Y)\Phi_k(Y)\rho(Y)dY \approx \sum_{\ell=1}^{L} w_\ell u(Y_\ell)\Phi_k(Y_\ell). \tag{6}$$

Sobol' sensitivity indices are obtained from HDMR expansion as [11]

$$\mathcal{S}_i = \frac{\text{var}[u_i]}{\text{var}[u(Y)]}. \tag{7}$$

The accuracy of Sobol' sensitivity indices depends on polynomial orders used in the subset gPCs. For this work, each subset is limited to first-order polynomials in each dimension, providing linear global sensitivities. While higher orders may reveal additional features, the linear expansion is much less expensive to calculate and provides a reasonable

analysis of the uncertainty space. For 17 inputs, only 34 BISON simulations were required, and the resulting end-of-life statistics were in good agreement with previous studies for this benchmark [12].

Time-dependent uncertainty analysis in RAVEN is performed using a snapshot approach: for each requested time step through the simulation, a HDMR expansion surrogate model is created for each response using the data reported from BISON. Interpolating between surrogates makes the collective time-dependent surrogate model. In this mode, it is critical to sample many time steps to provide accurate interpolation. Because the quadrature points needed to create the HDMR surrogates is the same at each time step, no additional BISON simulations are required to transition from steady-state to time-dependent uncertainty analysis. Uncertainty analysis was recorded at 100 equally-spaced burnup points between the beginning and end of life.

RESULTS

The evolution of the mean and variance of the four responses over burnup is given in Figs. 1-2. Each response is scaled linearly by the parameter shown in the legend. The nominal power shape in time is superimposed for reference.

From Figs. 3-6 the variance generally increases as the transients are simulated; however, some drops in the variance of the max centerline temperature warrant attention, in particular for Fig. 3. As seen in Figs. 2 and 3, variance spikes for centerline temperature near power changes in the transient. As seen in Fig. 1, immediately after each power drop, the max centerline temperature value drops significantly as well. Because the variance is dominated by the system power near the transients as shown in Fig. 2, the system power scaling factor is the chief source of variance. Since the uncertain parameter is a scaling factor, a reduction in the total power results in a smaller variance, which is reflected in the reduction in variance for the max centerline temperature immediately after transients as per Fig. 3. The peak in Fig. 6 corresponds to the variance introduced by the timing when the fuel expands to meet the clad. Because this time is dependent on the initial gap thickness, variance increases dramatically for the clad elongation depending on the thickness of the gap.

In Figs. 3-6, the evolution of sensitivities of various responses are shown with respect to increasing burnup. In addition, the power history used in the simulation is overlayed to provide insight in time-based changes. In each case, only the most significant uncertain inputs are shown for clarity. There are generally 4 significant events in the simulation cycle. The first occurs just after 1% fission per initial metal atom (FIMA), where the fuel has expanded enough to make contact with the clad. The remainder are near 0.02, 0.04, and 0.06 FIMA, where the system power drops.

The max fuel centerline temperature is taken at the axial center of the fuel pin. Sensitivity to the fuel conductivity dominates over most of the variance history as seen in Fig. 3; however, system power has more impact near gradients

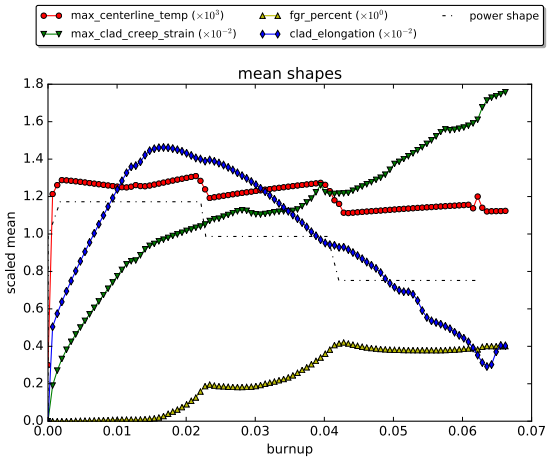

Fig. 1: Response Mean Values

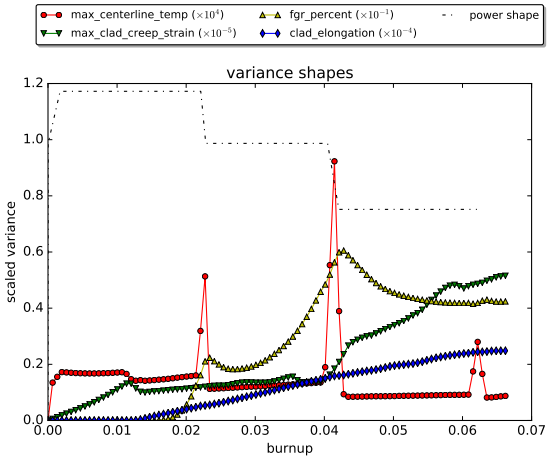

Fig. 2: Response Variance Values

in the power profile.

As expected, the clad creep rate is the most sensitive parameter for clad creep strain as shown in Fig. 4; however, it is interesting to note the rise and fall of the gap thickness as an important parameter in the middle of the burnup range.

Early in life the fission gas release is dependent on several parameters, which gives way to only the fuel conductivity and system power later. This can be seen in Fig. 5. The sensitivities in the variance of clad elongation have three distinct sections. At the beginning, clad elongation is perturbed most by clad conductivity, inlet temperature, and system power, with growing influence from fuel density. These are somewhat suddenly replaced by gap thickness, which then slowly trades places with clad creep rate over the remainder of the life cycle.

DISCUSSION

We have demonstrated HDMR and SCgPC in RAVEN used to perform time-dependent uncertainty propagation analysis in codes modeling transient behavior. Review-

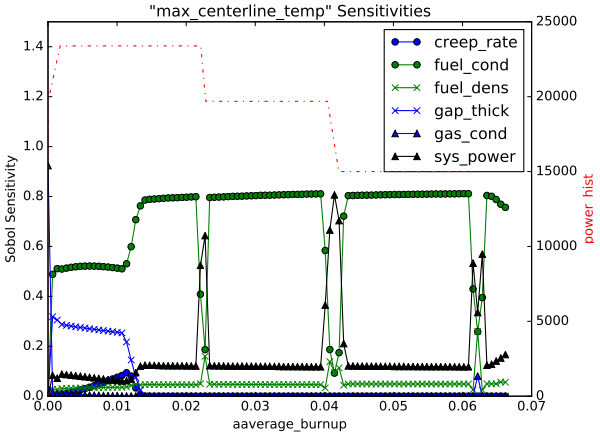

Fig. 3: Max Fuel Centerline Temperature

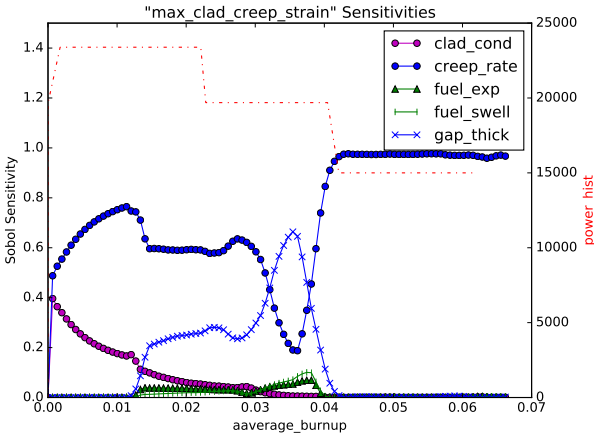

Fig. 4: Max Clad Creep Strain

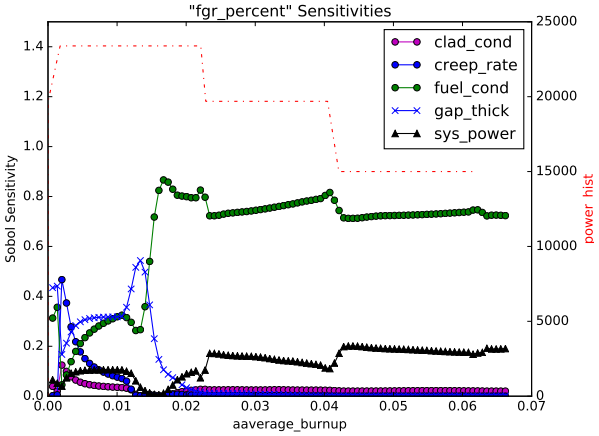

Fig. 5: Fission Gas Release (Percent)

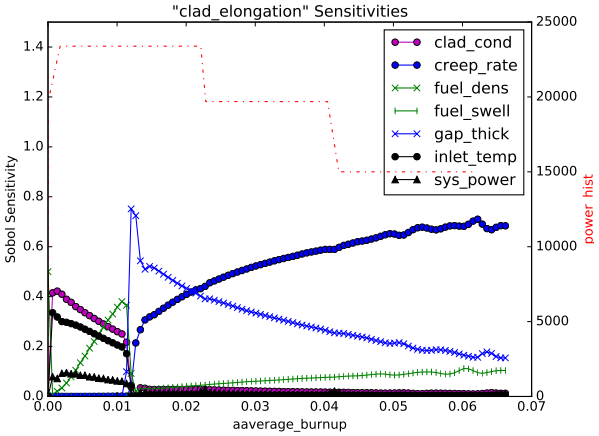

Fig. 6: Clad Elongation

ing the time-evolution of Sobol' sensitivities provides new methods in understanding the impact of uncertain input parameters as changes occur during the transient simulation. At small additional cost to static uncertainty propagation, transient analysis has valuable insights to offer.

REFERENCES

1. RABITI, COGLIATI, PASTORE, GARDNER, and ALFONSI, "Fuel reliability analysis using bison and raven," in "PSA 2015 Probabilistic Safety Assessment and Analysis," Sun Valley, Idaho (April 2015).
2. TALBOT and PRINJA, "Sparse-grid stochastic collocation uncertainty quantification convergence for multigroup diffusion," *2014 ANS winter conference transactions*, **111**, 747–750 (November 2014).
3. TALBOT, PRINJA, and RABITI, "Adaptive Sparse-Grid Stochastic Collocation Uncertainty Quantification Convergence for Multigroup Diffusion," *2016 ANS summer conference transactions*, **114**, 738–740 (June 2016).
4. TALBOT, WANG, and RABITI, "Multistep input reduction for high dimensional uncertainty quantification in RAVEN code," *2016 PHYSOR transactions* (May 2016).
5. RABITI, ALFONSI, MANDELLI, COGLIATI, and KINOSHITA, "RAVEN, a new software for dynamic risk analysis," in "PSAM 12 Probabilistic Safety Assessment and Management," Honolulu, Hawaii (June 2014).
6. BLYTH, PORTER, AVRAMOVA, IVANOV, ROYER, SARTORI, CABELLOS, FEROUKHI, and IVANOV, "Benchmark for uncertainty analysis in modelling (UAM) for design, operation, and safety analysis of LWRs. Volume II: specification and support data for the core cases (phase II)." *Nuclear Energy Agency/Nuclear Science Committee of the Organization for Economic Cooperation and Development*, **Version 2** (2014).
7. NEWMAN, HANSEN, and GASTON, "Three dimensional coupled simulation of thermomechanics, heat, and oxygen diffusion in nuclear fuel rods," *Journal of Nuclear Materials*, **392**, 1, 6 – 15 (2009).
8. AYRES and EATON, "Uncertainty quantification in nuclear criticality modelling using a high dimensional model representation," *Annals of Nuclear Energy*, **80**, 379–402 (May 2015).
9. LI, ROSENTHAL, and RABITZ, "High dimensional model representations," *J. Phys. Chem. A*, **105** (2001).
10. SMOLYAK, "Quadrature and interpolation formulas for tensor products of certain classes of functions," in "Dokl. Akad. Nauk SSSR," (1963), vol. 4, p. 123.
11. SOBOL, "On sensitivity estimation for nonlinear mathematical models," *Matematicheskoe Modelirovanie*, **2**, 112–118 (1990).
12. SWILER, GAMBLE, SCHMIDT, and WILLIAMSON, "Sensitivity Analysis of OECD Benchmark Tests in BISON," Tech. rep., Sandia National Laboratories (SNL-NM), Albuquerque, NM (United States) (2015).